



Optimal control of a fed-batch reactor with overflow metabolism

Carlos Martínez, Jean-Luc Gouzé

► To cite this version:

Carlos Martínez, Jean-Luc Gouzé. Optimal control of a fed-batch reactor with overflow metabolism. IFAC 2020 - 1st Virtual World Congress by the International Federation of Automatic Control, Jul 2020, Berlin / Virtual, Germany. hal-03130517

HAL Id: hal-03130517

<https://hal.science/hal-03130517>

Submitted on 3 Feb 2021

HAL is a multi-disciplinary open access archive for the deposit and dissemination of scientific research documents, whether they are published or not. The documents may come from teaching and research institutions in France or abroad, or from public or private research centers.

L'archive ouverte pluridisciplinaire **HAL**, est destinée au dépôt et à la diffusion de documents scientifiques de niveau recherche, publiés ou non, émanant des établissements d'enseignement et de recherche français ou étrangers, des laboratoires publics ou privés.

Optimal control of a fed-batch reactor with overflow metabolism

Carlos Martínez *

Jean-Luc Gouze †

Université Côte d’Azur, Inria, INRAE, CNRS, Sorbonne Université
Biocore team, Sophia Antipolis, France

February 3, 2021

Abstract Fast growing *E. coli* cells in glucose-aerobic conditions excrete fermentation by-products such as acetate. This phenomenon is known as overflow metabolism and can pose a major problem in industrial bio-processes. In this paper, we study optimal control strategies for feeding a fed-batch reactor subject to overflow metabolism. We consider that acetate has an inhibitor effect on the glucose uptake, and we also consider the cost associated to process duration. In our approach, using the Pontryagin Maximum Principle and numerical solutions we describe the optimal feeding policy that maximizes biomass productivity and minimizes the cost duration of the process. We show that a singular regime is possible, in which cells grow at a slow rate to prevent acetate formation. If the cost associated to the process is too high, only bang-bang solutions are allowed.

keywords: Dynamics and control; Industrial biotechnology; Fed-batch; Overflow metabolism

1 Introduction

Escherichia coli (*E. coli*) is a bacterium that is naturally found in the intestine of humans and other mammals. This bacterium plays an important role in the biotechnology industry for large-scale production of proteins for therapeutic use ([2]). Glucose is generally the preferred carbon source of *E. coli* ([6]), and depending on growth conditions, *E. coli* combines two different metabolic strategies to harvest energy from glucose, aerobic respiration (oxygen required) and/or fermentation (not oxygen required) ([9]). Respiration is more energy-efficient than fermentation. Nevertheless, in fast growing cells, some energy is obtained

*carlos.martinez@inria.fr

†jean-luc.gouze@inria.fr

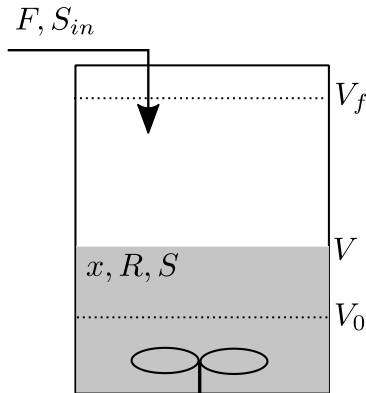


Figure 1: A schematic diagram of a simplified fed-batch reactor. The initial volume of the bacterial culture is V_0 . The volume increases as the fed-batch reactor is fed at a flow rate F with a concentration of glucose S_{in} . Feeding stops when the final volume V_f is reached. The evolution of the bulk concentrations of bacteria (X), glucose (S), and acetate (R) depend on the feeding rate F .

by fermentation, even in excess oxygen conditions. This phenomenon is referred as *overflow metabolism*. During fermentation (when overflow metabolism occurs), acetate is excreted to the medium as by-product. The accumulation of acetate has an inhibitory effect on cells growth ([13]), which can pose a major problem in microbial bioprocesses. Note that overflow metabolism has been observed in many microorganisms (see the book of [19]). For example, fast growing yeast excrete ethanol which can inhibit their growth.

Several studies suggest the existence of a threshold glucose uptake rate, above which overflow metabolism happens (see the work of [3] and the references therein). Thus, a straightforward strategy to increase biomass productivity, is to prevent acetate formation by forcing cells to uptake glucose from the medium below the threshold rate. This can be done in a fed-batch reactor restricting the feeding rate. Different authors have shown experimentally that this strategy leads to high density cultures (see for example the works of [12] and [1]). In the context of yeast cultures, this strategy have been used to construct adaptive controls or extremum seeking algorithms for increasing biomass productivity (see the works of [18] and [8]). One problem of this strategy, is that biomass is generated at a slower rate than the cells are capable of achieving. Therefore, the optimality of this strategy is not clear.

In this work, we investigate if maintaining the uptake rate of glucose at a rate that prevents the acetate formation is an optimal strategy in fed-batch reactors for the production of *E. coli*. In our approach, we study an optimal control problem with the criterion proposed by [16]. The criterion aims to maximize the quantity of bacteria at the end of the process, taking into account the cost associated to the process duration. To model *E. coli* growth, we consider a classical fed-batch reactor model and the recently proposed model by [14].

Thus, we consider the existence of a threshold glucose uptake rate, above which overflow metabolism happens, and consequently the excretion of acetate.

In the context of fed-batch processes (without overflow metabolism), several optimal feeding strategies, with respect to different criteria, have been determined by the use of the Pontryagin Maximum Principle (PMP) (see for examples the works of [15] and [17]). These strategies are of “bang-bang” type, singular, or a combination of both. In general, characterizing the optimal solution of optimal control problems is quite challenging. Numerical solutions are of great help in this context. To study our problem, we apply the PMP to obtain some insights into the form of a singular arc. Then, using the software BOCOP ([5]) (version 2.10), we obtain numerical simulations under different conditions. This approach allows us to characterize the optimal feeding strategies.

Our paper is organized as follows. In section 2, we describe the optimal control problem. In section 3, we apply the PMP, and we define a feedback control. In section 4, we solve numerically the optimal control problem and we describe the different structures of the optimal solutions. In section 5, we give some conclusions.

2 Problem formulation

We consider a fed-batch reactor (see Figure 1) with an *E. coli* population which density is denoted by x . This population grows at a specific growth rate $\mu(\cdot)$. The specific growth rate considers the carbon gain by glucose uptake and the carbon loss (in form of acetate) due to metabolic overflow *i.e.*

$$\mu(\cdot) = Y_S r_S(\cdot) - Y_R r_{of}(\cdot), \quad (1)$$

with r_S the glucose uptake rate, r_{of} the metabolic overflow rate (or acetate formation rate), and Y_S, Y_R yield coefficients. The glucose uptake rate depends on the glucose concentration (S) and on the acetate concentration (R):

$$r_S(S, R) = r_{S,max} \frac{S}{K_S + S} \frac{K_{i,R}}{K_{i,R} + R}, \quad (2)$$

where $r_{S,max}$ is the maximal glucose uptake rate, and $K_S, K_{i,R}$ are kinetic constants. Following [3], r_{of} depends on r_S *i.e.* $r_{of} = f(r_S)$, with f defined as (see Figure 2):

$$f(r_S) := k \max\{0, r_S - r_{S0}\}, \quad (3)$$

with $r_{S0} > 0$ the threshold glucose uptake rate above which acetate excretion occurs, and $k > 0$. We assume the following relation which is verified by the parameters estimated by [14]:

$$Y_S - kY_R > 0. \quad (4)$$

It is straightforward to verify that (4) implies $\frac{\partial \mu}{\partial S} > 0$ and $\frac{\partial \mu}{\partial R} < 0$. The growth of bacteria in the fed-batch reactor is modeled by :

$$\begin{aligned}
\frac{dx}{dt} &= \left(\mu(S, R) - \frac{F}{V} \right) x \\
\frac{dS}{dt} &= \frac{F}{V} (S_{in} - S) - r_S(S, R)x \\
\frac{dR}{dt} &= -\frac{F}{V} R + r_{of}(S, R)x \\
\frac{dV}{dt} &= F \\
x(0) &= x_0, S(0) = S_0, R(0) = R_0, \\
V(0) &= V_0, V(t_f) = V_f
\end{aligned} \tag{5}$$

Feed rate F is the control variable, and V is the volume. The initial values (at $t = 0$) of x, S, R and V are specified, as well as the final value of V (V_f). We want to maximize the total biomass production in the reactor together while minimizing the process duration. We consider the criterion proposed by [16]:

$$\begin{aligned}
\max_F \quad & x(t_f)V(t_f) - c_1 \int_{t_0}^{t_f} dt, \\
& 0 \leq F \leq F_{max},
\end{aligned} \tag{6}$$

where c_1 is a composite overall time cost in units of cell biomass per unit of time, and F_{max} is the maximal flow rate allowed in the system. The terminal time t_f is not fixed in this formulation.

3 Necessary optimality conditions

The classical PMP requires the continuous differentiability of the dynamics with respect to the state variables. In our model, overflow metabolism is described by the maximum function, which is not differentiable. Thus, to apply the PMP to (5)-(6), we consider a smooth approximation of f . Let δ be a positive real number, we define the function f_δ through the following properties (see Figure 2):

- $f_\delta(r_S) = 0$, for all $r_S \leq r_{S0}$,
- $f_\delta(r_S) > 0, f'_\delta(r_S) > 0$ for all $r_S \in (r_{S0}, r_{S0} + \delta)$,
- $f'_\delta(r_S) = k$ for all $r_S \geq r_{S0} + \delta$.

It is clear that $f_\delta \rightarrow f$ as $\delta \rightarrow 0^+$ uniformly. The necessary conditions for optimization of the problem (5)-(6), with f replaced by f_δ , are determined by the PMP. The associated Hamiltonian is given by:

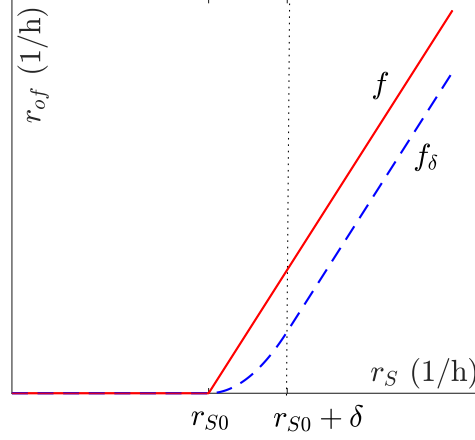


Figure 2: Functions f (continuous line) and f_δ (dash line). The function f (3) relates the acetate excretion rate (r_{of}) with the glucose uptake rate (r_S). The function f_δ (defined in Section 3) is a smooth approximation of f .

$$\begin{aligned}
H = & -c_1 + \lambda_x \left(Y_S r_S - Y_R f_\delta(r_S) - \frac{F}{V} \right) x \\
& + \lambda_S \left(\frac{F}{V} (S_{in} - S) - r_S x \right) \\
& + \lambda_R \left(-\frac{F}{V} R + f_\delta(r_S) x \right) + \lambda_V F.
\end{aligned} \tag{7}$$

For the adjoint variables, let us define $\Lambda_S = \lambda_S - Y_S \lambda_x$ and $\Lambda_R = \lambda_R - Y_R \lambda_x$. Then, for λ_x , λ_S , λ_R , and λ_V , the dynamics are given by:

$$\begin{aligned}
\frac{d\lambda_x}{dt} &= r_S \Lambda_S - f_\delta(r_S) \Lambda_R + \frac{F}{V} \lambda_x, \\
\frac{d\lambda_S}{dt} &= x \frac{\partial r_S}{\partial S} (\Lambda_S - f'_\delta(r_S) \Lambda_R) + \frac{F}{V} \lambda_S, \\
\frac{d\lambda_R}{dt} &= x \frac{\partial r_S}{\partial R} (\Lambda_S - f'_\delta(r_S) \Lambda_R) + \frac{F}{V} \lambda_R, \\
\frac{d\lambda_V}{dt} &= \frac{F}{V^2} (-\lambda_x x + \lambda_S (s_{in} - S) - \lambda_R R).
\end{aligned} \tag{8}$$

with $\lambda_x(t_f) = V_f$ and $\lambda_S(t_f) = \lambda_R(t_f) = 0$. Since the Hamiltonian is linear in the control variable (F), the structure of an optimal control \hat{F} is determined by the sign of the *switching function* $H_F := \frac{\partial H}{\partial F}$. Indeed,

$$\hat{F} = \begin{cases} F_{max} & \text{if } H_F > 0, \\ 0 & \text{if } H_F < 0, \end{cases}$$

with

$$H_F = \frac{1}{V} (-\lambda_x x + \lambda_S (S_{in} - S) - \lambda_R R) + \lambda_V. \tag{9}$$

If H_F vanishes over an interval of time I , a singular regime takes place. The following result gives necessary conditions for the existence of a singular regime.

Proposition 3.1. *Consider the problem (5)-(6) with f replaced by f_δ and assume that $S(0) \leq S_{in}$. If H_F (defined in (9)) vanishes in a sub-interval of time I , then:*

$$0 \leq r_S(t) - r_{S0} \leq \delta, \quad (10)$$

for all $t \in I$.

Proof. The proof is given in the Appendix. \square

Proposition 3.1 suggests that if an optimal trajectory of (5)-(6) presents a singular arc during a subinterval of time I , then $r_S(t) = r_{S0}$ for all $t \in I$ (take δ small enough in (10)). In such a case, the singular arc, denoted F_{sing} , satisfies $\frac{dr_S}{dt}|_{r_S=r_{S0}} = 0$ i.e.

$$F_{sing} = \frac{r_{S0}xV}{S_{in} - S + \frac{SR(K_S+S)}{K_S(K_{iR}+R)}}. \quad (11)$$

As we will show in the next section, F_{sing} can be a singular arc of the optimal solution of (5)-(6). To end this section, based on F_{sing} , we define a feedback control \tilde{F} that will be useful for describing the structure of optimal controls in the next section:

$$\tilde{F} = \begin{cases} 0 & \text{if } r_S > r_{S0} \text{ or } V \geq V_f, \\ \min\{F_{max}, F_{sing}\} & \text{if } r_S \leq r_{S0} \text{ and } V < V_f. \end{cases} \quad (12)$$

If the feedback control \tilde{F} is applied when $r_S > r_{S0}$ and $V < V_f$, then the reactor will be operated in batch mode ($F = 0$), which results in a decrease of r_S . The batch mode stops when r_S equals r_{S0} . After that, $\tilde{F} = F_{sing}$ and r_S remains equal to r_{S0} provided $F_{sing} \leq F_{max}$. If \tilde{F} switches from F_{sing} to F_{max} ($F_{sing} > F_{max}$ and $V < V_f$), then r_S decreases. Thus, r_S remains equal than or lower than r_{S0} until the final volume (V_f) is achieved. Then, the reactor is operated again in batch mode. This feeding strategy (\tilde{F}) is comparable to that proposed by [12]. As we will see in the next section, in some cases \tilde{F} corresponds to an optimal control.

4 Structure of the optimal control

We solve numerically the problem (5)-(6) for different values of S_0 , x_0 , and c_1 , with parameters from Table 1. We use a direct method implemented in the software BOCOP ([5]) (version 2.10). The problem is discretized by a two-stage Gauss-Legendre method of order 4 with 300 time steps. We consider a constant initialization, and the tolerance for IPOPT NLP solver is set at 10^{-12} .

Figure 3 shows the optimal control strategy for different initial conditions and values of c_1 . For brevity, we only show some plots representing the different structures that were observed. To describe the different solutions we recall the feedback control \tilde{F} defined in (12). If $x_0 = 0.1 \text{ g/L}$, $S_0 = 20 \text{ g/L}$, and $c_1 = 0.1 \text{ g/h}$ (Figure 3A), the optimal control coincides with the feedback control \tilde{F} during all the process duration. If $x_0 = 0.1 \text{ g/L}$, $S_0 = 0 \text{ g/L}$, and $c_1 = 0.1 \text{ g/h}$

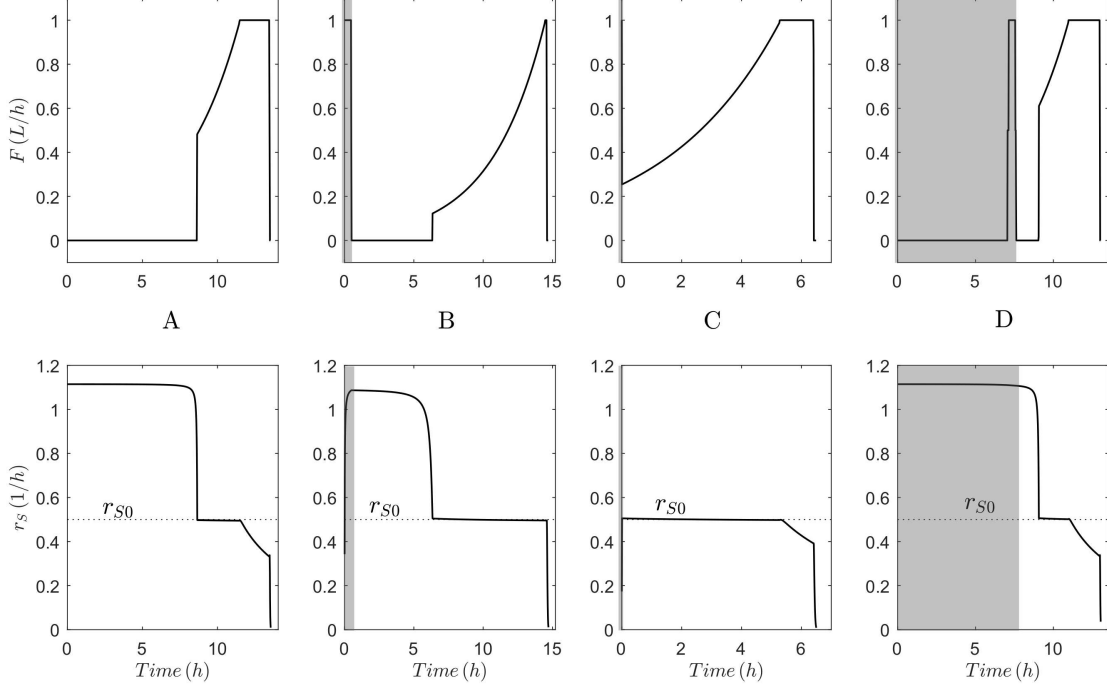


Figure 3: Optimal solution of the problem (5)-(6) for different values of S_0 , x_0 , and c_1 . The not-shaded area represents the interval of time while the control \tilde{F} (defined in (12)) is applied. Parameters are taken from Table 1 **A.** $S_0 = 20 \text{ g/L}$, $x_0 = 0.1 \text{ g/L}$, and $c_1 = 0.1 \text{ g/h}$. **B.** $S_0 = 0 \text{ g/L}$, $x_0 = 0.1 \text{ g/L}$, and $c_1 = 0.1 \text{ g/h}$. **C.** $S_0 = 0 \text{ g/L}$, $x_0 = 5 \text{ g/L}$, and $c_1 = 0.1 \text{ g/h}$. **D.** $S_0 = 20 \text{ g/L}$, $x_0 = 0.1 \text{ g/L}$, and $c_1 = 0.5 \text{ g/h}$.

(Figure 3B), the feeding rate is maximum during the first 30 minutes, and then the feedback control \tilde{F} is applied until the final time. If $x_0 = 5 \text{ g/L}$, $S_0 = 0 \text{ g/L}$, and $c_1 = 0.1 \text{ g/h}$ (Figure 3C), then during a very short period of time the flow rate is maximum. During this time, the value of r_S increases from 0 to r_{S0} . Then, the feedback control \tilde{F} is applied until the end, keeping almost all the time the glucose uptake rate set to r_{S0} . If $x_0 = 0.1 \text{ g/L}$, $S_0 = 20 \text{ g/L}$, and $c_1 = 0.5 \text{ g/h}$ (Figure 3D), a bang-bang control, switching from 0 to F_{max} , is observed during the startup. Then, the control switches from F_{max} to \tilde{F} , and \tilde{F} is applied until the final time.

Figures 4 and 5 show the optimal profile of the optimal control for different values of S_0 and c_1 . Figure 4 shows that as c_1 increases, a singular regime occurs during a shorter interval of time, and a bang-bang solution (during the startup,

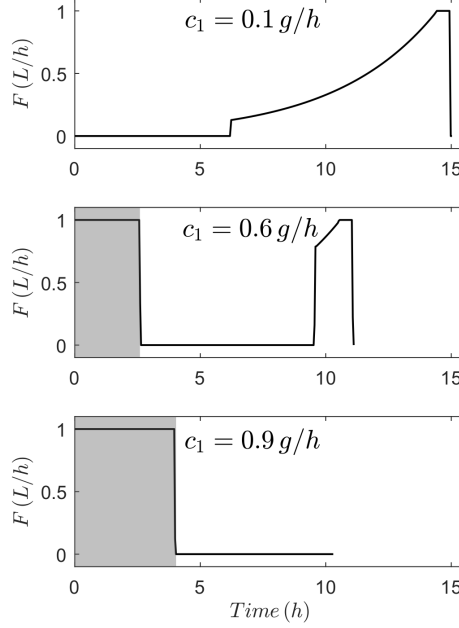


Figure 4: Optimal feeding profile for different values of c_1 . The not-shaded area represents the interval of time while the control \tilde{F} (defined in (12)) is applied. Parameters are taken from Table 1 ($S_0 = 5 \text{ g/L}$ and $x_0 = 0.1 \text{ g/L}$)

shaded area), switching from F_{max} to 0, occurs during a longer time. For values of c_1 equal than or higher than 0.9 g/L , there is not singular arc. Similarly to Figure 4, Figure 5 shows the same effect when increasing c_1 . However, the bang-bang solution associated to c_1 during the startup, switches from 0 to F_{max} .

Numerical simulations suggest the existence of a time $t^* \in [0, t_f)$ (the end of the shaded areas in Figures 3, 4, and 5), such that the feedback control \tilde{F} is applied from the time t^* until the final time (not-shaded areas in Figures 3, 4, and 5). If $t^* > 0$, during the interval of time $[0, t^*]$, the optimal control is equal to F_{max} (Figures 3B and 3C) or is bang-bang, switching from 0 to F_{max} (Figure 3D). If $t^* = 0$, the optimal control coincides with \tilde{F} (Figure 3A). As shown in Figures 4 and 5, the value of t^* is related to the value of c_1 . Indeed, if c_1 is too high, \tilde{F} is only applied when the final volume is reached (Figures 4 and 5).

Table 2 shows the biomass productivity and the cost duration associated to Figures 4 and 5. Biomass productivity does not change very much with changes on c_1 . This is probably due to the initial and final volumes. Unfortunately, we did not obtain convergence of the numerical method for large volumes to test this hypothesis.

Table 1: Parameters and initial conditions.

Parameter	Value	Unit	Remark
$r_{S,max}$	1.12	h^{-1}	[10]
K_S	0.1	g/L	[10]
$K_{i,R}$	4	g/L	[10]
k	0.25	—	
r_{S0}	0.5	h^{-1}	
Y_S	0.52	gX/gS	[21]
Y_R	0.4	gX/gR	[10]
c_1	0.1 – 1.2	g/h	
S_{in}	10	g/L	
F_{max}	1	L/h	
V_0	1	L	
V_f	5	L	
x_0	0.1 – 5	g/L	
S_0	0 – 20	g/L	
R_0	1	g/L	

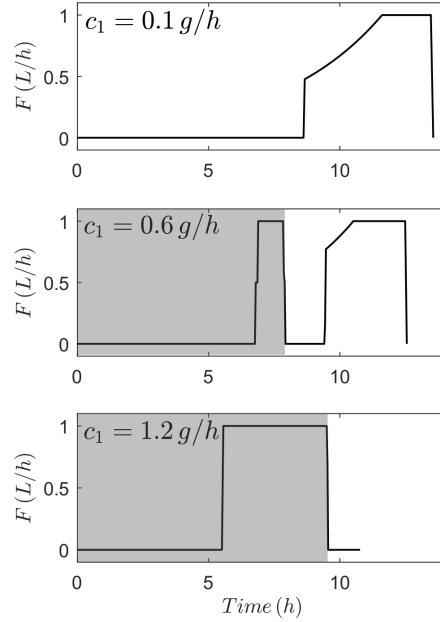


Figure 5: Optimal feeding profile for different values of c_1 . The not-shaded area represents the interval of time while the control \tilde{F} (defined in (12)) is applied. Kinetic parameters are taken from Table 1 ($S_0 = 20 g/L$ and $x_0 = 0.1 g/L$).

Table 2: Biomass production ($x(t_f)V_f$) and cost associated to process duration ($c_1 \int_{t_0}^{t_f} dt$) for the different conditions represented in Figures 4 and 5.

	c_1 (g/h)	$x(t_f)V_f$ (g)	$c_1 \int_{t_0}^{t_f} dt$ (g)
Figure 4	0.1	23.3	1.6
	0.6	22.2	7.3
	0.9	21.25	10
Figure 5	0.1	30.7	1.6
	0.6	29.7	8.3
	1.2	28.7	14.8

5 Conclusions and future work

The optimal feeding rate changes with the initial conditions, x_0 and S_0 , and the process duration cost, c_1 . In some cases, the optimal feeding rate is given by the feedback optimal control (\hat{F}). This control prevents acetate formation by forcing cells to uptake glucose from the medium below the threshold uptake rate (r_{S0}), even if biomass is generated at a slower rate than the cells are capable of achieving. This confirms that the simple strategy proposed by [12] may be optimal. However, as the cost associated to the process duration increases, the optimal feeding strategy combines an initial bang-bang control with the feedback control. This is explained by the fact that for a high operational cost, it is convenient to accelerate the process by feeding at maximal rate. Indeed, if the operational cost is heavily weighted, the optimal solutions are of bang-bang type, which is consistent with the results of [7]. Feeding at maximal rate during the startup is not necessarily associated to high operational cost, but to a small initial glucose uptake rate. Feeding at maximal rate during the startup may be necessary to increase the glucose uptake rate to a level equal than or higher than the critical uptake rate (r_{S0}), so that the feedback control \hat{F} is optimal for the rest of the process.

As a future work, we will consider the acetate consumption. According to [20], *E. coli* can consume acetate, but only after the glucose is totally consumed. Another future work, follows the works of [11] and [4]. It considers a consortium with another *E. coli* strain that grows on consuming acetate.

Appendix

Here we prove Proposition 3.1. We recall the notations of Section 3. If H_F vanishes during a sub-interval of time, then $\frac{dH_F}{dt} = 0$. Let us define $W = \Lambda_S - f'_\delta(r_S)\Lambda_R$. It can be shown that:

$$\frac{dH_F}{dt} = \frac{x}{V} W \left((S_{in} - S) \frac{\partial r_S}{\partial S} - R \frac{\partial r_S}{\partial R} \right).$$

Assume that $S < S_{in}$. Since $\frac{\partial r_S}{\partial S} > 0$ and $\frac{\partial r_S}{\partial R} < 0$, the sign of W determines the monotonicity of H_F . The derivative of W with respect to the time gives:

$$\begin{aligned} \frac{dW}{dt} &= -\Lambda f''_{\delta}(r_S) \frac{dr_S}{dt} \\ &+ W \left(x \frac{\partial r_S}{\partial S} + \frac{F}{V} - x f'_{\delta}(r_S) \frac{\partial r_S}{\partial R} \right) \\ &+ (r_S \Lambda_S - f_{\delta}(r_S) \Lambda_R) (Y_R f'_{\delta}(r_S) - Y_S). \end{aligned} \quad (13)$$

Lemma 5.1. *Let us define $\alpha = x[f_{\delta}(r_S) - r_S f'_{\delta}(r_S)]$ and $S(0) \leq S_{in}$. If $H_F = 0$ in a sub-interval of time I , then for all $t \in I$:*

a) $\alpha(t) \neq 0$,

b) $\Lambda_R(t) = \frac{c_1}{\alpha(t)x(t)}$.

Proof. If $H_F = 0$ in a sub-interval of time, then $\frac{dH_F}{dt} = W = 0$. Then, $A\lambda = b$, with A given by

$$\begin{bmatrix} \left(\mu - \frac{F}{V}\right)x & \frac{F}{V}(S_{in} - S) - r_S x & -\frac{F}{V}R + f_{\delta}(r_S)x & F \\ -x & S_{in} - S & -R & V \\ Y_R f'_{\delta}(r_S) - Y_S & 1 & -f'_{\delta}(r_S) & 0 \end{bmatrix},$$

$\lambda = [\lambda_x, \lambda_S, \lambda_R, \lambda_V]^T$, and $b = [c_1, 0, 0]^T$. If $\alpha = 0$, the equality $A\lambda = b$ leads to $c_1 = 0$, which is a contradiction. Thus, a) is proved. Now, for $\alpha \neq 0$, any solution of $A\lambda = b$ satisfies $\lambda_R = \frac{c_1}{x[f_{\delta}(r_S) - r_S f'_{\delta}(r_S)]} + Y_R \lambda_x$. From where the proof b) follows. \square

Lemma 5.2. *If $S(0) \leq S_{in}$ and $H_F = 0$ during a sub-interval of time, then $f''_{\delta}(r_S) > 0$.*

Proof. By contradiction, let us assume that $H_F = 0$ and $f''_{\delta}(r_S) = 0$. In view of Lemma 5.1, necessarily $f'_{\delta}(r_S) = k$. Since $W = 0$, we obtain that $\Lambda_S = k\Lambda_R$. Recalling (13), we have:

$$\frac{dW}{dt} = \Lambda_R(kr_S - f_{\delta}(r_S))(Y_R k - Y_S).$$

From Lemma 5.1 and (4), we obtain that:

$$\frac{dW}{dt} = -\frac{c_1}{x}(Y_R f'_{\delta}(r_S) - Y_S) > 0.$$

This contradicts the fact that $W = 0$. \square

Proof. (Proposition 3.1) It follows from Lemmas 5.1 and 5.2. \square

References

- [1] KR Babu, S Swaminathan, S Marten, N Khanna, and U Rinas. Production of interferon- α in high cell density cultures of recombinant *Escherichia coli* and its single step purification from refolded inclusion body proteins. *Applied microbiology and biotechnology*, 53(6):655–660, 2000.
- [2] Mohammed N Baeshen, Ahmed M Al-Hejin, Roop S Bora, MM Ahmed, HA Ramadan, Kulvinder S Saini, Nabih A Baeshen, and Elrashdy M Redwan. Production of biopharmaceuticals in *E. coli*: current scenario and future perspectives. *J Microbiol Biotechnol*, 25(7):953–962, 2015.
- [3] Markus Basan, Sheng Hui, Hiroyuki Okano, Zhongge Zhang, Yang Shen, James R Williamson, and Terence Hwa. Overflow metabolism in *Escherichia coli* results from efficient proteome allocation. *Nature*, 528(7580):99, 2015.
- [4] Hans C Bernstein, Steven D Paulson, and Ross P Carlson. Synthetic *Escherichia coli* consortia engineered for syntrophy demonstrate enhanced biomass productivity. *Journal of biotechnology*, 157(1):159–166, 2012.
- [5] JF Bonnans, V Grelard, and P Martinon. Bocop, the optimal control solver, open source toolbox for optimal control problems. URL <http://bocop.org>, 2011.
- [6] Anat Bren, Junyoung O Park, Benjamin D Towbin, Erez Dekel, Joshua D Rabinowitz, and Uri Alon. Glucose becomes one of the worst carbon sources for *E. coli* on poor nitrogen sources due to suboptimal levels of cAMP. *Scientific reports*, 6:24834, 2016.
- [7] Lorenzo Cazzador. On the optimal control of fed-batch reactors with substrate-inhibited kinetics. *Biotechnology and bioengineering*, 31(7):670–674, 1988.
- [8] L Dewasme, B Srinivasan, M Perrier, and A Vande Wouwer. Extremum-seeking algorithm design for fed-batch cultures of microorganisms with overflow metabolism. *Journal of Process Control*, 21(7):1092–1104, 2011.
- [9] Luca Gerosa, Bart RB Haverkorn van Rijsewijk, Dimitris Christodoulou, Karl Kochanowski, Thomas SB Schmidt, Elad Noor, and Uwe Sauer. Pseudo-transition analysis identifies the key regulators of dynamic metabolic adaptations from steady-state data. *Cell systems*, 1(4):270–282, 2015.
- [10] Maria Jesus Guardia and Eloy Garcia Calvo. Modeling of *Escherichia coli* growth and acetate formation under different operational conditions. *Enzyme and microbial technology*, 29(6-7):449–455, 2001.

- [11] Emily Harvey, Jeffrey Heys, and Tomáš Gedeon. Quantifying the effects of the division of labor in metabolic pathways. *Journal of theoretical biology*, 360:222–242, 2014.
- [12] DJ Korz, U Rinas, K Hellmuth, EA Sanders, and W-D Deckwer. Simple fed-batch technique for high cell density cultivation of *Escherichia coli*. *Journal of biotechnology*, 39(1):59–65, 1995.
- [13] Gregory W Luli and WILLIAM R Strohl. Comparison of growth, acetate production, and acetate inhibition of *Escherichia coli* strains in batch and fed-batch fermentations. *Appl. Environ. Microbiol.*, 56(4):1004–1011, 1990.
- [14] Marco Mauri, Jean-Luc Gouzé, Hidde De Jong, and Eugenio Cinquemani. Enhanced production of heterologous proteins by a synthetic microbial community: Conditions and trade-offs. *PLOS Computational Biology*, 16(4):e1007795, 2020.
- [15] Seujeung Park and W Fred Ramirez. Optimal production of secreted protein in fed-batch reactors. *AIChE Journal*, 34(9):1550–1558, 1988.
- [16] Ka Yiu San and Gregory Stephanopoulos. A note on the optimality criteria for maximum biomass production in a fed-batch fermentor. *Biotechnol. Bioeng.:(United States)*, 26(10), 1984.
- [17] Ka-Yiu San and Gregory Stephanopoulos. Optimization of fed-batch penicillin fermentation: A case of singular optimal control with state constraints. *Biotechnology and bioengineering*, 34(1):72–78, 1989.
- [18] S Valentinotti, B Srinivasan, Ulf Holmberg, D Bonvin, C Cannizzaro, M Rhiel, and U Von Stockar. Optimal operation of fed-batch fermentations via adaptive control of overflow metabolite. *Control engineering practice*, 11(6):665–674, 2003.
- [19] Alexei Vazquez. *Overflow metabolism: from yeast to marathon runners*. Academic Press, 2017.
- [20] Alan J Wolfe. The acetate switch. *Microbiol. Mol. Biol. Rev.*, 69(1):12–50, 2005.
- [21] Bo Xu, Mehmedalija Jahic, and Sven-Olof Enfors. Modeling of overflow metabolism in batch and fed-batch cultures of *Escherichia coli*. *Biotechnology progress*, 15(1):81–90, 1999.